

Published in final edited form as:

Biorheology. 2010 ; 47(3-4): 193–203. doi:10.3233/BIR-2010-0570.

Drag-reducing polymers diminish near-wall concentration of platelets in microchannel blood flow

R. Zhao^a, J.N. Marhefka^{a,c,*}, J.F. Antaki^{b,c}, and M.V. Kameneva^{a,c,d,**}

^aMcGowan Institute for Regenerative Medicine, University of Pittsburgh, Pittsburgh, PA, USA

^bDepartment of Biomedical Engineering, Carnegie Mellon University, Pittsburgh, PA, USA

^cDepartment of Bioengineering, University of Pittsburgh, Pittsburgh, PA, USA

^dDepartment of Surgery, University of Pittsburgh, Pittsburgh, PA, USA

Abstract

The accumulation of platelets near the blood vessel wall or artificial surface is an important factor in the cascade of events responsible for coagulation and/or thrombosis. In small blood vessels and flow channels this phenomenon has been attributed to the blood phase separation that creates a red blood cell (RBC)-poor layer near the wall. We hypothesized that blood soluble drag-reducing polymers (DRP), which were previously shown to lessen the near-wall RBC depletion layer in small channels, may consequently reduce the near-wall platelet excess. This study investigated the effects of DRP on the lateral distribution of platelet-sized fluorescent particles (diam. = 2 μm , $2.5 \times 10^8/\text{ml}$) in a glass square microchannel (width and depth = 100 μm). RBC suspensions in PBS were mixed with particles and driven through the microchannel at flow rates of 6–18 ml/h with and without added DRP (10 ppm of PEO, MW = 4500 kDa). Microscopic flow visualization revealed an elevated concentration of particles in the near-wall region for the control samples at all tested flow rates (between 2.4 ± 0.8 times at 6 ml/h and 3.3 ± 0.3 times at 18 ml/h). The addition of a minute concentration of DRP virtually eliminated the near-wall particle excess, effectively resulting in their even distribution across the channel, suggesting a potentially significant role of DRP in managing and mitigating thrombosis.

Keywords

Drag-reducing polymers; platelet margination; microchannels; red blood cell traffic

1. Introduction

Platelet margination is known to be an important factor contributing to coagulation and/or thrombosis within small blood vessels as well as medical devices containing small channels, junctions and gaps [1–3]. Extensive experimental studies have been conducted to investigate the effects of various independent parameters (such as hematocrit, flow rate, particle size) on this phenomenon under physiological conditions *in vitro* [19–21]. Those studies showed that platelet transport in blood flow is regulated by both diffusion and convection [2,8,7,29,37], and that platelet diffusivity can be enhanced by the presence of red blood cells (RBC) [2,31].

© 2010 – IOS Press and the authors. All rights reserved

** Address for correspondence: Dr. Marina Kameneva, 450 Technology Dr., Suite 300, Pittsburgh, PA 15219, USA. Tel.: +1 412 624 5281 (office); +1 412 624 5283 (laboratory); Fax: +1 412 624 5363; kamenevamv@upmc.edu.

* Dr. Marhefka's current affiliation is National Institute of Standards and Technology, Gaithersburg, MD, USA.

Possible mechanisms include *exclusion* and *shear-induced mixing* [1,2,6,12,17]. The *exclusion* mechanism refers to the expulsion of platelets towards the wall by the RBC as they migrate towards the vessel centerline – a phenomenon which is typically observed in blood vessels and microchannels with a diameter below 300 μm (Fåhræus effect). The *shear-induced mixing* mechanism refers to a local enhancement of platelet diffusivity caused by the rotation and random motion of RBC in the shear field.

Our recent studies also demonstrated the occurrence of platelet-sized particle margination at supra-physiological shear stress conditions, representative of blood flow within medical devices such as cardiopulmonary support systems and renal dialysis. Flow visualization within microchannels (2 cm \times 100 μm \times 100 μm) revealed a platelet near-wall excess up to about 800% at the highest shear stress studied (\sim 200 Pa) [36]. This observation is particularly relevant to devices containing small channels, junctions or gaps, in which near-wall shear forces and foreign surface contact can cause platelet activation or damage – resulting in thrombosis and/or aggravating coagulopathy [29,32]. Therefore, development and utilization of methods for decreasing platelet margination could be beneficial for improved biocompatibility of prosthetic blood-wetted devices.

Drag-reducing polymers (DRP) are a special class of soluble polymers with long-chain molecular structure and molecular weight above 1000 kDa that may significantly decrease the resistance to turbulent flow in a pipe when added in minute concentrations [30]. This phenomenon, known as the Toms effect, was discovered over 60 years ago, although the mechanism is still not fully understood. Over the past several decades DRP have been tested for numerous industrial applications such as pipeline transport of crude oil, firefighting and reducing drag on ships and submarines [3,9,16]. However, their quick mechanical degradation significantly impaired widespread use of these polymers in industry. While DRP have been studied in numerous engineering areas, they are not widely known in the biomedical field. However, blood-soluble DRP added to blood at minute concentrations have been found to produce significant beneficial effects on blood circulation by increasing blood flow, tissue perfusion and tissue oxygenation, and reducing vascular resistance in experimental animals [4,14,15,18,23,26,28]. These polymers, including polyethylene oxide (PEO), polyacrylamide (PAM) and natural DRP such as hyaluronic acid and those extracted from okra or Aloe vera, have been found to significantly increase the survival of rats subjected to acute hemorrhagic shock [5,18,22,24], improve the microcirculation in diabetic rats [13] and reduce the development of atherosclerosis [10,11,25].

The mechanism of the intravascular effect of DRP is particularly noteworthy considering the absence of turbulent flow in vascular systems, hence excluding the possibility of the Toms phenomenon. Nevertheless, the fact that similar beneficial effects can be obtained with polymers of varied chemical structures suggests that the mechanism of their effect on blood circulation is based on hydrodynamic principles rather than biochemical pathways [18].

Recent studies by our group discovered that minute concentrations (few parts per million) of blood soluble DRP can significantly reduce or even eliminate the RBC free layer in microchannels with a diameter of 100 μm [18,23,27]. We hypothesized that this elimination of the RBC free layer may also reduce the near-wall platelet concentration in small channels or vessels. To test this hypothesis, we extended the previous microchannel studies to include the measurement of the concentration of platelet-sized fluorescent particles within the RBC suspensions under similar flow conditions.

2. Methods section

2.1. Sample preparation

Fresh bovine blood anticoagulated with EDTA was centrifuged at 3500 RPM for 10 minutes and the plasma and buffy coat were discarded. RBC were washed three times in phosphate buffered saline (PBS) (P4417, Sigma-Aldrich Corp., St. Louis, MO, USA) containing 1% bovine albumin (A7284, Sigma-Aldrich Corp., St. Louis, MO, USA). The washed RBC were resuspended in PBS with 1% bovine albumin at 40% hematocrit (Ht). The RBC suspension was divided into two equal parts. PEO (molecular weight 4500 kDa, Polyox WSR-301, Dow Chemical, Midland, MI, USA) was added to one part at a final concentration of 10 $\mu\text{g/ml}$ (10 ppm) and slowly mixed for one hour to make a PEO sample. An equal volume of PBS was added to the other RBC suspension to make a control sample. The asymptotic viscosity of the prepared RBC suspensions was measured using a capillary viscometer (CANNON Instrument Company, State College, PA, USA) at ambient temperature ($21 \pm 1^\circ\text{C}$) and was found to be comparable in samples without and with DRP additives (3.21 ± 0.21 cP vs. 3.40 ± 0.19 cP, respectively, at shear rates above 400 s^{-1}). Normal RBC morphology was confirmed using light microscopy.

A suspension of platelet-sized fluorescent polystyrene particles (R0200, Duke Scientific Corporation, Palo Alto, CA, USA) with a mean diameter of 2 μm , a light excitation peak of 542 nm, emission peak of 612 nm, and initial concentration of 2.3×10^9 particles/ml was added to both samples to achieve a bulk concentration of 2.5×10^8 particles/ml, which is within the physiological range of platelet concentration in bovine blood ($1\text{--}4 \times 10^8$ particles/ml). The final hematocrit of the RBC suspension was 36%. The preparations were mixed for 30 minutes in plastic centrifuge tubes on a rocker plate just prior to introduction into the microchannels.

2.2. Experimental setup

A schematic of the experimental setup is shown in Fig. 1a. A square glass microchannel (Vitrocells, VitroCom Inc., Mountain Lakes, NJ, USA) with a length of 2 cm, a cross section (inside dimensions) of $100 \times 100 \mu\text{m}$, and a wall thickness of 50 μm was placed through a small transparent holder and glued on the two ends. The holder was then attached to a transparent flow chamber. The microchannel was connected to the inflow and outflow tubing with two holes (ID = 3 mm) which were drilled on the flow chamber (Fig. 1b). Samples were pumped through the microchannel at flow rates of 6–18 ml/h by a syringe pump (KDS 100, KD Scientific Inc., Holliston, MA, USA). The flow was fast enough to avoid significant RBC sedimentation. The samples were collected in a small reservoir that was open to the atmosphere. The flow chamber was adhered to the stage of an inverted microscope (IX70, Olympus, Melville, NY, USA) equipped with a 20 \times objective with a depth of field of 6 μm (LCPlanFL, 20 \times , NA = 0.40, Olympus, Melville, NY, USA). The microflow system was routinely calibrated with saline prior to each test in terms of pressure transducers, flow rates and microchannel diameter. Pressure transducers were calibrated (zeroed) against atmospheric pressure and known pressure using a calibrated manometer, and the flow rate was verified by measuring it using a stopwatch.

An Nd:YAG laser (Solo PIV I-15, New Wave Research, Inc., Fremont, CA, USA) with a pulse duration of 3–5 ns was used to illuminate the blood flow within the channel. A high-sensitivity CCD camera (PCO Sensicam QE double exposure, The Cooke Corp., Romulus, MI, USA) was used to capture magnified images of fluorescent particles within the microchannel while the images of red blood cells were eliminated by an HQ filter set (Series 41002, Exciter: HQ535/50 \times ; Dichroic: Q565LP; Emitter: HQ610/75m; Croma Technology Corp., Bellows Falls, VT, USA) which was placed in the filter turret of the microscope. A

series of images (688 × 520 pixels) was recorded to observe the lateral distribution of the platelet-sized fluorescent particles in the microchannel by synchronizing the laser and the camera using a pulse generator (BK Precision 3011B, Maxtec International Corp., Chicago, IL, USA) with a frame rate less than 4 Hz to assure complete replacement of the cell population in each image. The image layer was located about 5 μm above the bottom of the microchannel. No cells attached to the microchannel surface were visualized. One hundred such images were recorded at each flow rate and 3 trials were conducted. The region of interest was chosen at least 1 cm from the microchannel inlet to avoid entrance effects. A more detailed description of this experimental setup is given in our previous report [35].

2.3. Image processing

The concentration profile of platelet-sized particles was determined with a custom-written image analysis program using Matlab (Mathworks, Natick, MA, USA). Figure 2 provides a flowchart of the image processing procedure. The images were first cropped to isolate the region of the microchannel. The background was then homogenized to equilibrate uneven illumination and the image contrast was enhanced by histogram stretching. The minimal and maximal intensity values in this process were carefully selected according to the original intensity histogram. The particles in the image were identified by thresholding followed by erosion to eliminate spurious noise. The threshold was adjusted to minimize the difference between numbers of manually and automatically counted particles. This process was repeated for five random frames and the same threshold was used thereafter.

2.4. Data analysis

The microchannel image was partitioned into 20 evenly distributed, 5 μm wide, bands in the lateral direction (Fig. 3). The number of particles in each band was counted by the custom-written analysis program described above and averaged over 100 images. The concentration profile of the platelet-sized particles was then normalized as

$$C(r) = \frac{(\# \text{particles in RoI}) / (\text{total volume of RoI})}{(\text{bulk particle count} / \text{unit volume})},$$

where $C(r)$ denotes the relative concentration, indicating the ratio of particle concentration in the region of interest (RoI) to the bulk particle concentration of 2.5×10^8 particles/ml. The volume associated with the RoI was estimated based on the depth of field specifications of the objective (=6 μm).

To describe the kinetics of the samples in an approximate way and to scale the experimental results for comparison to other conditions, the blood samples were assumed to be incompressible Newtonian fluids. A closed form solution of Navier–Stokes equation for a fully developed flow in a rectangular duct [33] was used to obtain the velocity profile, from which the wall shear rate was calculated. At flow rates of 6–18 ml/h, the average wall shear rates were ~ 3000 – 9000 s^{-1} , and the corresponding Reynolds numbers were ~ 8 – 25 .

The Student's t -test was used to evaluate differences between the observed particle concentrations in the control and DRP groups. A value of $p < 0.05$ was assumed to indicate statistical significance.

3. Results and discussion

Figure 4 shows the raw images as well as the relative particle concentration for control and DRP samples at the flow rate of 18 ml/h ($Re = 25$). In control suspensions, the elevated near-wall particle concentration was clearly visible, reaching a maximum of about 3.3 ± 0.3

at the flow rate of 18 ml/h. The platelet margination phenomenon was observed at all tested flow rates (6–18 ml/h) in the control group (Fig. 5), increasing with flow rate from 2.4 ± 0.8 times at 6 ml/h to 3.3 ± 0.3 times at the flow rate of 18 ml/h. These observations are in agreement with previous studies of Eckstein et al. in microtubes which reported a near-wall excess of approximately 200–800% using 2–3 μm particles in microchannels of 135–220 μm diameter and hematocrit of 40% [32,34].

In contrast, the RBC suspensions containing DRP (10 ppm PEO) demonstrated no identifiable excess, with virtually uniform concentration across the channel (Fig. 5). Since the focal plane was $\sim 5 \mu\text{m}$ above the bottom of the microchannel, there were more particles observed in control samples than in the DRP group across the channel due to the particle margination near the bottom surface in the vertical direction. The difference in near-wall concentration (up to 15 μm from the wall) between the two groups was statistically significant ($p < 0.05$).

For the first time, the current study demonstrated that the platelet margination phenomenon in an RBC suspension flowing in a glass square microchannel was eliminated by adding a small concentration of DRP (10 ppm). Since our previous study using particle suspensions with and without RBC [36] demonstrated that RBC were responsible for the elevated near-wall concentration of platelet-sized particles, the remarkable effectiveness of blood soluble DRP to virtually eliminate platelet margination can most likely be explained through the influence of the added DRP on RBC traffic in microchannels, a phenomenon previously documented [18]. Although the precise physical mechanism of the discovered effect remains to be fully understood, it is reasonable to believe that blood soluble DRP could potentially be used to reduce the risk of thrombosis related to near-wall platelet accumulation in small vessels and blood-wetted devices.

3.1. Study limitations

Experimental errors could largely be introduced by automatic image processing. This error was evaluated by randomly selecting 5 images in each experimental setting and comparing the difference between the average automatic and manual particle counts. The error was minimized to within 10% by tuning the image processing parameters. Since this is a subjective measure, it may introduce a source of systematic error. A related source of error is the counting of particles out of the focal plane. These unfocused particles may erroneously be counted either manually or automatically. However, these artifacts were reduced in the current experiments because the high concentration of RBC blocked most of the unfocused particles. In addition, a function to eliminate extremely large particles was added to the image processing program to reduce the erroneous counting of out of focus particles since these particles look larger than those in focus. This source of systematic error should not affect the primary conclusions of this study.

A study with images taken at various depths could provide more information on the particle concentration distribution in the depth direction. However, in RBC suspensions with a high hematocrit (e.g., 36% in our study), RBC block the visualization of regions far from the microchannel bottom. Future studies using ghost RBC may help to resolve this issue.

4. Conclusions

Using a microscopic visualization technique, the current study demonstrated that adding a minute concentration of soluble DRP to flowing blood significantly reduced or eliminated near-wall platelet accumulation in small tubes. The basic mechanism behind this DRP effect is related to the previously demonstrated ability of DRP to affect traffic of RBC in microchannels *in vitro* and microvessels *in vivo* preventing RBC relocation away from the

wall, thus reducing the expulsion of platelets towards the wall and minimizing space available for accumulation of platelets or platelet-sized particles. The presence of DRP in blood can be potentially utilized to reduce platelet damage and the occurrence of thrombosis *in vivo*.

Acknowledgments

The authors acknowledge the assistance provided by Mr. Skicki, former undergraduate student at the Bioengineering Department, University of Pittsburgh. This research was supported in part by NIH grant R01 HL089456-01.

Appendix: Matlab program for image processing

<code>im = imread("image.tif")</code>	import an image named "image.tif";
<code>ima = im(1:520, wall_x1:wall_x2)</code>	image crop; wall_x1 and wall_x2 are the coordinates of the channel walls;
<code>se = strel("disk", 7)</code>	reduce uneven illumination;
<code>j = imtophat(ima, se)</code>	reduce uneven illumination;
<code>imb = imadjust(j, stretchlim(j),[0 1])</code>	improve image quality by stretching the histogram;
<code>level = graythresh(imb)</code>	setup gray level to convert to binary image;
<code>bw = im2bw(imb, level)</code>	convert to binary image;
<code>k = imopen(bw, strel("disk", 2))</code>	eliminate small points, which are considered as noise;
<code>L = bwlabel(k,4)</code>	
<code>stats = imfeature(L, "Centroid")</code>	show the centroid of particles;
<code>allCentroid = [stats.Centroid].</code>	

References

1. Aarts PA, Bolhuis PA, Sakariassen KS, et al. Red blood cell size is important for adherence of blood platelets to artery subendothelium. *Blood* 1983;62:214–217. [PubMed: 6860793]
2. Aarts PA, Heethaar RM, Sixma JJ. Red blood cell deformability influences platelets – vessel wall interaction in flowing blood. *Blood* 1984;64:1228–1233. [PubMed: 6498337]
3. Burger ED, Chorn LG, Perkins TK. Studies of drag reduction conducted over a broad range of pipeline conditions when flowing Prudhoe Bay crude oil. *J. Rheol* 1980;24:603.
4. Coleman PB, Ottenbreit BT, Polimeni PI. Effects of a drag-reducing polyelectrolyte of microscopic linear dimension (Separan AP-273) on rat hemodynamics. *Circ. Res* 1987;61:787–796. [PubMed: 3677337]
5. Cotoia A, Kameneva MV, Marascalco PJ, et al. Drag-reducing hyaluronic acid increases survival in profoundly hemorrhaged rats. *Shock* 2009;31:258–261. [PubMed: 18650778]
6. Eckstein EC, Belgacem F. Model of platelet transport in flowing blood with drift and diffusion terms. *Biophys. J* 1991;60:53–69. [PubMed: 1883945]
7. Eckstein EC, Koleski JF, Waters CM. Concentration profiles of 1 and 2.5 microns beads during blood flow. Hematocrit effects. *ASAIO Trans* 1989;35:188–190. [PubMed: 2597441]
8. Eckstein EC, Tilles AW, Millero FJ 3rd. Conditions for the occurrence of large near-wall excesses of small particles during blood flow. *Microvasc. Res* 1988;36:31–39. [PubMed: 3185301]
9. Fabula, AG.; Lumley, JL.; Taylor, WD. *Some Interpretations of the Toms Effect*. New York: Academic Press; 1966.
10. Faruqui FI, Otten MD, Polimeni PI. Protection against atherogenesis with the polymer drag-reducing agent Separan AP-30. *Circulation* 1987;75:627–635. [PubMed: 3815772]
11. Gannushkina IV, Antelava AL, Baranchikova MV. Diminished experimental alimentary atherogenesis under the influence of polymers that decrease the hydrodynamic resistance of the blood. *Bull. Exp. Biol. Med* 1993;116:367–370.

12. Goldsmith HL, Turitto VT. Rheological aspects of thrombosis and haemostasis: basic principles and applications. ICTH-Report – Subcommittee on Rheology of the International Committee on Thrombosis and Haemostasis. *Thromb. Haemost* 1986;55:415–435. [PubMed: 3750272]
13. Golub AS, Grigoryan SS, Kameneva MV, et al. Influence of polyethylene oxide on the capillary blood flow of diabetic rats. *Sov. Phys. Dokl* 1987;32:620.
14. Grigorian SS, Kameneva MV, Shakhnazarov AA. Effect of high molecular weight compounds dissolved in blood on hemodynamics. *Sov. Phys. Dokl. (Fluid Mech.)* 1976;21:702–703.
15. Grigorian, SS.; Kameneva, MV. Resistance-reducing polymers in the blood circulation. In: Chernyi, GG.; Regier, SA., editors. *Contemporary Problems of Biomechanics*. Boca Raton, FL: CRC Press; 1990. p. 99-110.
16. Hoyt JW. The effect of additives on fluid friction. *Trans. ASME J. Basic Eng* 1972;94:258–285.
17. Jordan A, David T, Homer-Vanniasinkam S, et al. The effects of margination and red cell augmented platelet diffusivity on platelet adhesion in complex flow. *Biorheology* 2004;41:641–653. [PubMed: 15477670]
18. Kameneva MV, Wu ZJ, Uraysh A, et al. Blood soluble drag-reducing polymers prevent lethality from hemorrhagic shock in acute animal experiments. *Biorheology* 2004;41:53–64. [PubMed: 14967890]
19. Karino T, Goldsmith HL. Flow behaviour of blood cells and rigid spheres in an annular vortex. *Philos. Trans. R. Soc. Lond. B Biol. Sci* 1977;279:413–445. [PubMed: 19795]
20. Karino T, Goldsmith HL. Adhesion of human platelets to collagen on the walls distal to a tubular expansion. *Microvasc. Res* 1979;17:238–262. [PubMed: 459938]
21. Karino T, Goldsmith HL. Role of blood cell-wall interactions in thrombogenesis and atherogenesis: a microrheological study. *Biorheology* 1984;21:587–601. [PubMed: 6487769]
22. Macias CA, Kameneva MV, Tenhunen JJ, et al. Survival in a rat model of lethal hemorrhagic shock is prolonged following resuscitation with a small volume of a solution containing a drag-reducing polymer derived from aloe vera. *Shock* 2004;22:151–156. [PubMed: 15257088]
23. Marhefka JN, Zhao R, Wu ZJ, et al. Drag reducing polymers improve tissue perfusion via modification of the RBC traffic in microvessels. *Biorheology* 2009;46:281–292. [PubMed: 19721190]
24. McCloskey CA, Kameneva MV, Uryash A, et al. Tissue hypoxia activates JMK in the liver during hemorrhagic shock. *Shock* 2004;22:380–386. [PubMed: 15377896]
25. Mostardi RA, Thomas LC, Greene HL, et al. Suppression of atherosclerosis in rabbits using drag reducing polymers. *Biorheology* 1978;15:1–14. [PubMed: 678620]
26. Pacella JJ, Kameneva MV, Lavery LL, et al. A novel hydrodynamic method for microvascular flow enhancement. *Biorheology* 2009;46:293–308. [PubMed: 19721191]
27. Pacella JJ, Kameneva MV, Villanueva FS. Drag reducing polymers improve coronary flow reserve through modulation of capillary resistance. *Biorheology* 2009;46:365–378. [PubMed: 19940353]
28. Polimeni PI, Ottenbreit BT. Hemodynamic effects of a poly(ethylene oxide) drag-reducing polymer, Polyox WSR N-60K, in the open-chest rat. *J. Cardiovasc. Pharmacol* 1989;14:374–380. [PubMed: 2476615]
29. Tilles AW, Eckstein EC. The near-wall excess of platelet-sized particles in blood flow: its dependence on hematocrit and wall shear rate. *Microvasc. Res* 1987;33:211–223. [PubMed: 3587076]
30. Toms, BA. Some observations on the flow of linear polymer solution through straight tubes at large Reynolds numbers. *1st Int. Congr. Rheology*; Amsterdam, Netherlands. 1948.
31. van Breugel HF, de Groot PG, Heethaar RM, Sixma JJ. Role of plasma viscosity in platelet adhesion. *Blood* 1992;80:953–959. [PubMed: 1498335]
32. Waters CM, Eckstein EC. Concentration profiles of platelet-sized latex beads for conditions relevant to hollow-fiber hemodialyzers. *Artif. Organs* 1990;14:7–13. [PubMed: 2302078]
33. White, FM. *Viscous Fluid Flow*. New York: McGraw-Hill; 1991. p. 1-736.
34. Yeh C, Eckstein EC. Transient lateral transport of platelet-sized particles in flowing blood suspensions. *Biophys. J* 1994;66:1706–1716. [PubMed: 8061219]

35. Zhao, R. PhD thesis. Pittsburgh, PA: Carnegie Mellon University; 2008. Experimental and theoretical investigation of blood flow dynamics associated with blood contacting devices.
36. Zhao R, Kameneva MV, Antaki JF. Investigation of platelet margination phenomena at elevated shear stress. *Biorheology* 2007;44:161–177. [PubMed: 17851165]
37. Zhao R, Marhefka JN, Shu F, et al. Micro-flow visualization of red blood cell-enhanced platelet concentration at sudden expansion. *Ann. Biomed. Eng* 2008;36:1130–1141. [PubMed: 18418710]

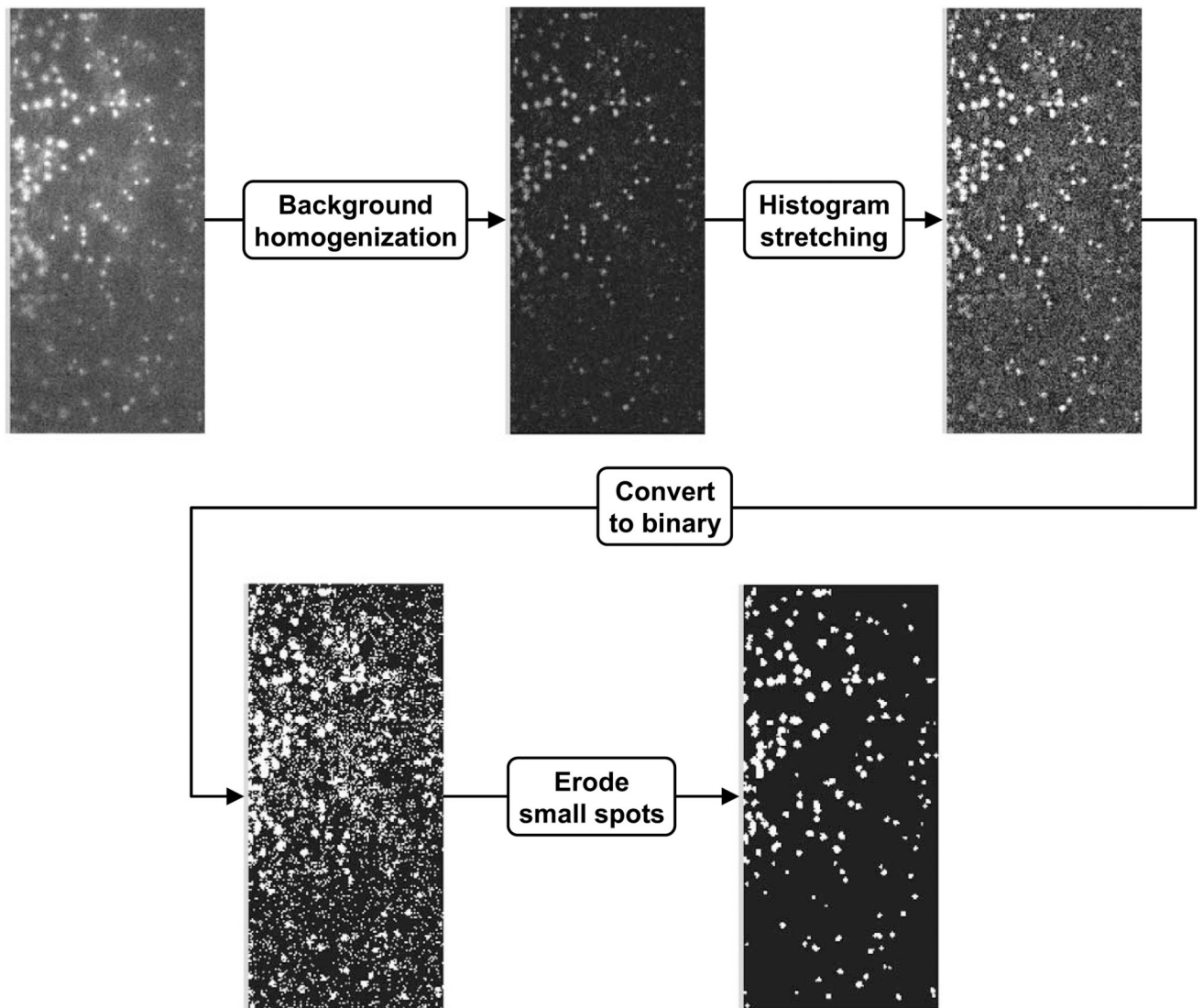


Fig. 2. Flowchart of image processing. The background of the image was homogenized to equilibrate uneven illumination and the image contrast was enhanced by histogram stretching. The particles in the image were identified by thresholding followed by erosion to eliminate spurious noise.

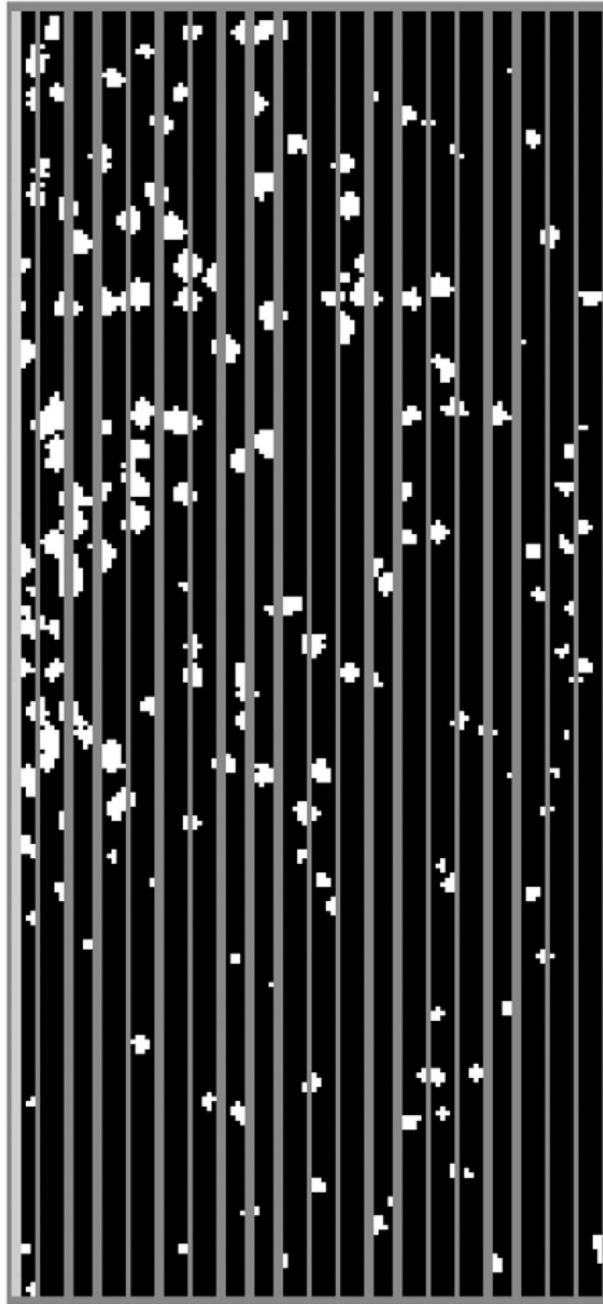


Fig. 3.
Image partition.

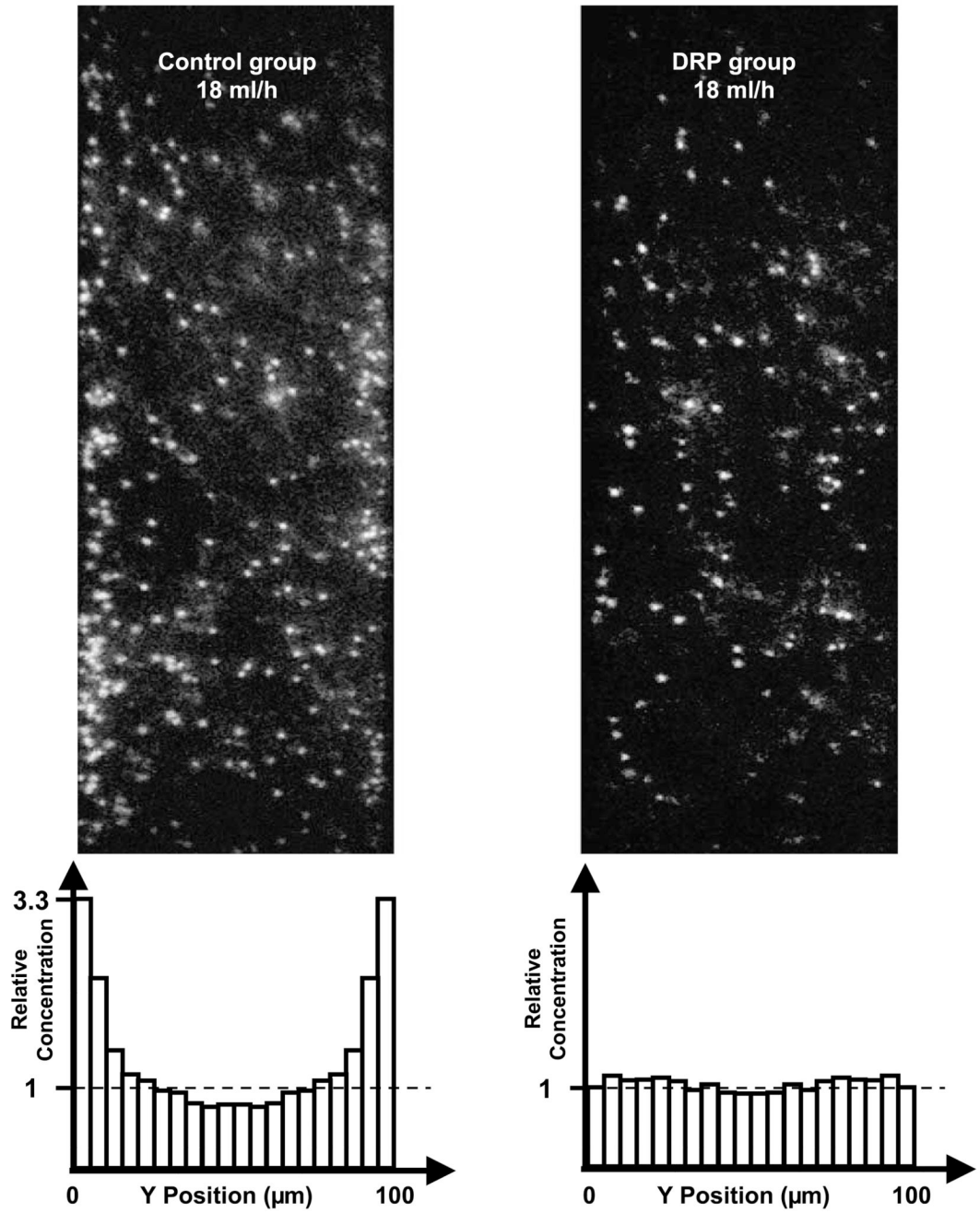


Fig. 4. Concentration profiles and representative images of relative concentration of platelet sized particles in RBC suspension (Ht = 36%, flow rate 18 ml/h). Left: control sample; right: DRP sample (with 10 ppm PEO); top: raw images; bottom: histograms of relative concentration averaged from 100 images.

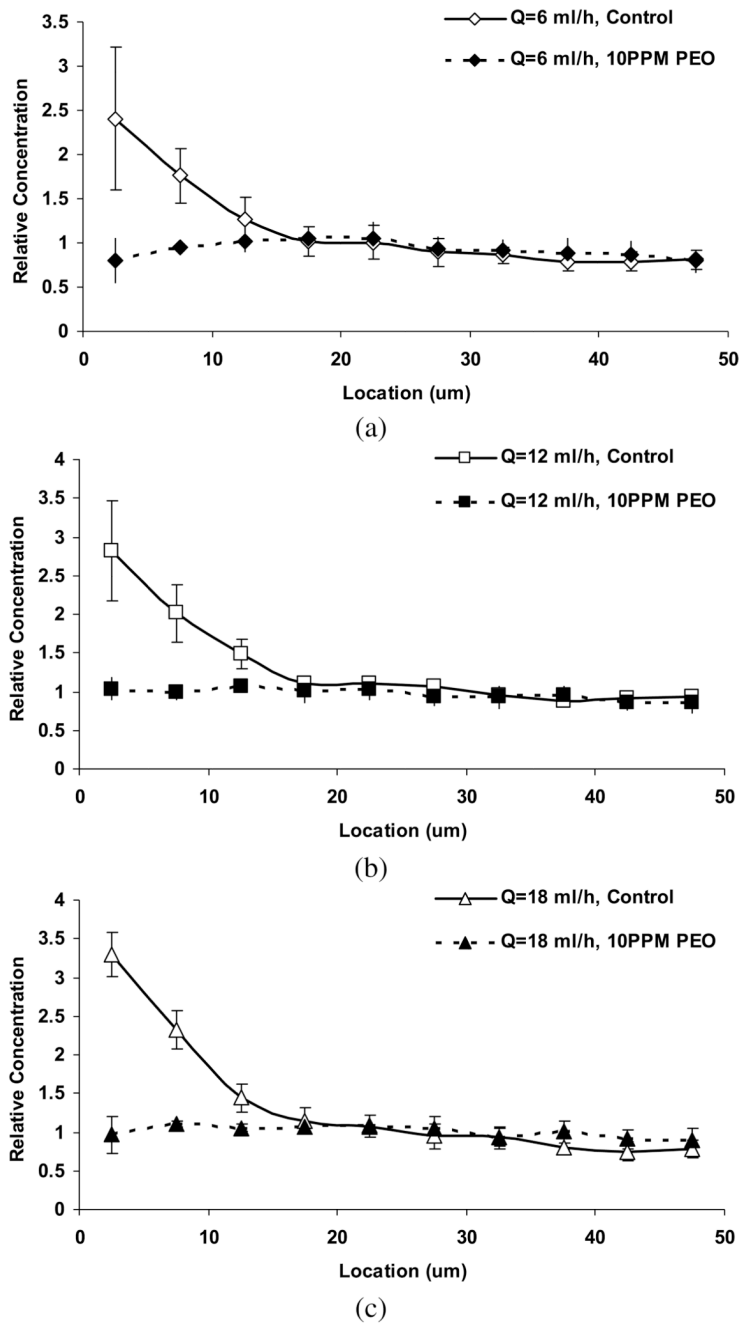


Fig. 5. Relative concentration of platelet-sized particles in RBC suspension (Ht = 36%) at various flow rates: 6 ml/h (a); 12 ml/h (b); 18 ml/h (c). The near-wall concentration (within the distance of 15 μm from the wall) was found to be statistically different between the two groups ($p < 0.05$).